Journal of Luminescence 131 (2011) 2451–2456

Contents lists available at ScienceDirect

Journal of Luminescence

journal homepage: www.elsevier.com/locate/jlumin

Preparation and characterization of Tb^{3+} and $Tb(sal)_3 \cdot nH_2O$ doped PC:PMMA blend

Y. Dwivedi [a], A.K. Singh [b], Rajiv Prakash [b], S.B. Rai [a,*]

[a] Laser and Spectroscopy Laboratory, Department of Physics, Banaras Hindu University, Varanasi 221005, India
[b] School of Material Science and Technology, Institute of Technology, Banaras Hindu University, Varanasi 221005, India

ARTICLE INFO

Article history:
Received 10 October 2010
Received in revised form
21 May 2011
Accepted 24 May 2011
Available online 22 June 2011

Keywords:
Energy transfer
Lanthanide
PC:PMMA blend
Optical property
Time resolved spectroscopy

ABSTRACT

Tb doped polycarbonate:poly(methyl methacrylate) (Tb–PC:PMMA) blend was prepared with varying proportions of PC and PMMA. Thermal and spectroscopic properties of the doped polymer have been investigated employing Fourier Transform Infrared (FTIR) absorption and differential scanning calorimetric (DSC) techniques. PC:PMMA blend (with 10 wt% PC and 90 wt% PMMA) shows better miscibility. Optical properties of the dopant Tb^{3+} ions have been investigated using UV–vis absorption and fluorescence excited by 355 nm radiation. It is seen that luminescence intensity of Tb^{3+} ion depends on PC:PMMA ratio and on Tb^{3+} ion concentration. Concentration quenching is seen for $TbCl_3 \cdot 6H_2O$ concentration larger than 4 wt%. Addition of salicylic acid to the polymer blend increases the luminescence from Tb^{3+} ions. Luminescence decay curve analysis affirms the non-radiative energy transfer from salicylic acid to Tb^{3+} ions, which is identified as the reason behind this enhancement.

1. Introduction

Considering the wide applicability of rare earth (RE) doped polymers, their compactness, efficiency and low cost, these materials have been the subject of intense investigation [1]. RE doped polymers have several advantages, viz. flexibility of shape, thickness and size and high electro-optic and thermo-optic coefficients [2,3]. The high luminescence efficiency from RE doped polymer combined with high color purity of emission may permit for next generation phosphor screens and display devices [4].

The scientific and technological interests in acrylic materials have grown considerably due to their excellent resistance to UV radiation and hydrolysis, which makes them useful for outdoor applications [5]. These polymers prevent segregation of dopent cations due to the coordination of the carboxylic groups with the metallic ions; hence these are a convenient matrix to incorporate cations.

Poly(methyl methacrylate) (PMMA) exhibits excellent transparency in the visible region of the spectrum and is also compatible with additives and plasticizers but suffers from brittleness and high water sensitivity. Copolymerization and polymer blending have been studied to combine the attractive features of each blend component while avoiding their drawback characteristics [6–8]. Among various blends of PMMA studied for miscibility a mixture of PMMA and polycarbonate (PC) has been of considerable interest in view of the excellent properties of PC, including ductility, low water absorption and high glass transition temperature. Different methods have been used to prepare these polymer blends, including solution casting, co-precipitation and melt mixing. The two polymers PMMA and PC have very different chemical structures; for example, PMMA has an aliphatic backbone and ester side-chain while PC is polyester of an aliphatic or aromatic dihydroxy compound, carbonic acid containing an ester backbone and polyurethane with an amino ester backbone. As a result, their refractive index, optical loss, and mechanical and thermal properties differ considerably.

Viville et al. [9] have shown that PC and PMMA are partially miscible due to the formation of an n–p complex between the PMMA ester group and the phenyl ring of PC. Agari et al. [6] obtained PC:PMMA blends that are a single-phase system under low critical solution temperature (180–220 °C) depending on the compositions by a simple solution casting method. Solvent effect on the morphology of PC:PMMA films have been discussed by Kyu and Saldanha [10], who suggest that the morphology is mostly controlled by a competition between a tendency of phase-separation and the process of solvent induced crystallization. Recently, Bonzanini et al. [11,12] have shown that PC:PMMA blends can serve as a host for RE based luminescent materials.

The present work is divided into two parts—the initial part is devoted to the preparation and structural characterization of bisphenol A polycarbonate, poly(methyl methacrylate) and their blend, using DSC and FTIR techniques while the second part of the paper deals with the optical characterization of PC, PMMA and

* Corresponding author. Tel.: +91 542 230 7308; fax: +91 542 2369889.
E-mail address: sbrai49@yahoo.co.in (S.B. Rai).

0022-2313/$ - see front matter © 2011 Elsevier B.V. All rights reserved.
doi:10.1016/j.jlumin.2011.05.063

PC:PMMA blend doped with Tb^{3+} ion and Tb–salicylic acid (Sal) by UV–vis absorption and fluorescence spectroscopy. Luminescence dynamics and energy transfer process have been investigated with the measurement of time resolved fluorescence.

2. Experimental

2.1. Material and methods

Poly(methyl methacrylate) (M.W. 15,000), bisphenol A polycarbonate (M.W. 10,000) and 99.9% pure Terbium chloride ($TbCl_3 \cdot 6H_2O$) are used as starting materials for sample preparation.

PC:PMMA blend containing different weight ratios of PC and PMMA were prepared by the solution casting method. Tetrahydrofuran (THF) was used as mutual solvent for all the blend compositions. Polymer fractions (by wt%) 100:0, 40:60, 20:80, 10:90 and 0:100 of PC and PMMA (these are denoted as PC:0 PMMA, PC:60 PMMA, PC:80 PMMA, PC:90 PMMA and PC:100 PMMA later on) are dissolved in THF at 45 °C and homogenized for 4 h in a closed environment followed by sonication for 10–15 min. The solutions are then poured in covered Petri dishes for controlled evaporation. Finally the samples were dried in a vacuum oven at 70 °C for removal of remaining solvents. Samples containing 1, 2, 4, 6, 8 wt% of [$TbCl_3 \cdot 6H_2O$] and 4 wt% $TbCl_3 \cdot 6H_2O$+3 wt% salicylic acid (Sal) were also prepared using the same procedure.

For the synthesis of $Tb(sal)_3 \cdot nH_2O$ complex doped in PC:PMMA blend, initially 12 mmole of salicylic acid was dissolved in 40 ml of distilled water and stirred with 15 ml of 1 M NaOH. To this solution 4 mmole of $TbCl_3 \cdot 6H_2O$ dissolved in 15 ml of distilled water was added slowly. Instantaneously the precipitate of $Tb(sal)_3 \cdot nH_2O$ was formed, which was dried in vacuum oven at 50 °C overnight. The complex thus formed was mixed with the tetrahydrofuran (THF) solution of PC:PMMA polymer and then dried. The films thus formed were stored in sample boxes at room temperature.

2.2. Measurements

Thermal analysis of undoped and codoped polymer samples was carried out using a differential scanning calorimetry (DSC; Mettler Toledo, 823) system at a heating rate of 10 °C/ min under nitrogen atmosphere. UV–vis absorption has been measured in the 200–900 nm range on a UV–vis spectrometer (Lambda 25, Perkin Elmer, Germany) while IR absorption has been measured in the 400–4000 cm^{-1} region using a double beam FTIR spectrometer Perkin Elmer RX1 with a resolution of 2 cm^{-1}.

For photoluminescence studies 355 nm radiation from a Nd:YAG laser (Spitlight 600, Innolas, Germany) was used for excitation and the luminescence emission was recorded using an iHR 0.32 m monochromator (Horiba JY, USA) equipped with a PMT (R1454) as detector. The luminescence decay was recorded using the third harmonic (355 nm) from a pulsed Nd:YAG laser (~20 mJ, 7 ns pulse width operating at 10 Hz) and a 150 MHz oscilloscope (model no. HM1507, Hameg Instruments).

3. Results and discussion

3.1. Thermal studies

DSC thermograms of Tb^{3+} ion dispersed in PC:PMMA blends were recorded during the second heating scan (initially samples were heated up to 300 °C and then allowed to cool at room temperature; thereafter samples were reheated up to 300 °C) and are shown in Fig. 1. Two different T_g are observed: one at ~106 °C and the other at ~148 °C in Tb–PC:60 PMMA. The two T_g correspond to T_g of pure PMMA and pure PC, respectively, showing immiscible blend formation. For other compositions, e.g. PC:80PMMA and PC:90PMMA, only one T_g at 106 and 105 °C, respectively, is seen, indicating that at these compositions (low PC), the blend behaves as a homogeneous blend.

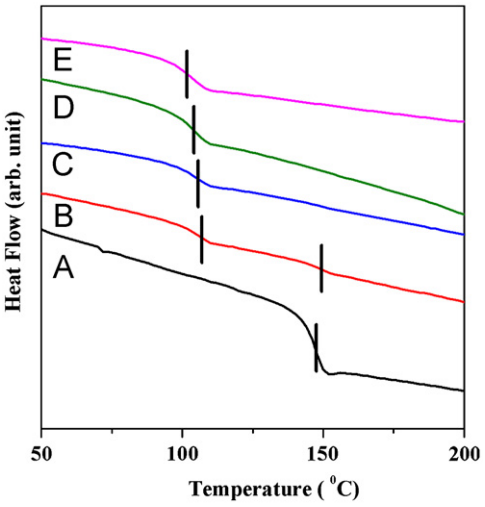

Fig. 1. DSC thermograms of quenched Tb^{3+} doped PC:PMMA blends: [A] PC+2% $TbCl_3 \cdot 6H_2O$, [B] PC:60PMMA+2% $TbCl_3 \cdot 6H_2O$, [C] PC:80PMMA+2% $TbCl_3 \cdot 6H_2O$, [D] PC:90PMMA+2% $TbCl_3 \cdot 6H_2O$, and [E] PMMA+2% $TbCl_3 \cdot 6H_2O$.

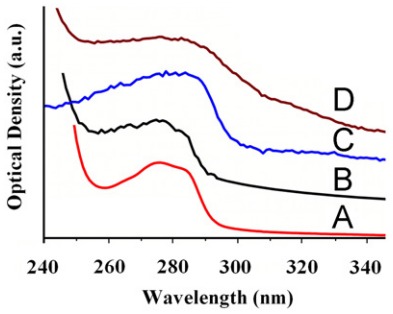

Fig. 2. UV–vis absorption spectra of [A] PMMA, [B] PC, [C] PC:90 PMMA, and [D] Tb–PC:90 PMMA.

3.2. Spectroscopic studies

3.2.1. Absorption spectroscopy

The optical absorption spectra of PC, PMMA and their blends containing different proportions of PC and PMMA doped with Tb ions have been recorded in the range of UV–vis region (200–900 nm) in particular to check the formation of blend and the presence of Tb^{3+} ions in the polymeric matrix [Fig. 2].

Two absorption peaks are seen for pure PC at 226 and 276 nm. Similarly for pure PMMA the absorption peaks are at 216 and 274 nm. These bands are ascribed to a $\pi \rightarrow \pi^*$ transition (smaller wavelength peak) and $n \rightarrow \pi^*$ transition (longer wavelength peak) of the C=O group. It is noticed that the presence of Tb ion causes a small shift. The peak at 288 nm is now seen at 291 nm [curves C and D of Fig. 2]. This change is a symptom of disturbance in local structure and is expected due to the interaction of Tb ions with the host especially to the carbonyl group. Formation of C=O—Tb—O=C like structures is probably the manner of these interactions. When Tb ion interacts with the carbonyl group the electron density of the C=O bond is reduced, which causes redshifting of

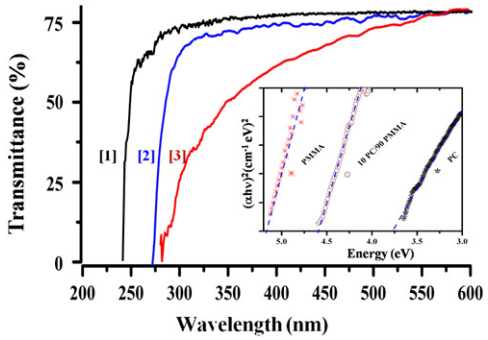

Fig. 3. Transmittance spectra of [1] PMMA, [2] PC:90 PMMA blend, and [3] PC. Inset shows Tauc's plot of the PMMA, PC:90PMMA and PC.

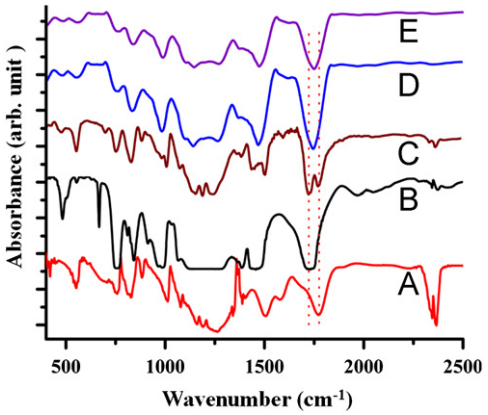

Fig. 4. FTIR absorption spectra of: [A] Pure PC, [B] Pure PMMA, [C] PC:60PMMA, [D] PC:90PMMA, and [E] 4Tb:PC:90PMMA.

the band. The above result indicates that the Tb^{3+} ions interact with PC: PMMA blend and mainly interact with the carbonyl group of the PC: PMMA blend.

Additionally, the absorption band at 288 nm is broadened in the presence of Tb ion. Several intraconfigurational (4f–4f) absorption peaks corresponding to Tb^{3+} ions were reported in literature in the wavelength range of 270–370 nm [13]. These peaks were expected to be buried in the broad absorption band of PC:PMMA blend and are not resolved though, due to the presence of Tb ion, absorption band of the blend gets broadened.

The UV–vis optical transmission spectra of pure PMMA, pure PC and PC:PMMA blends were also recorded to estimate the effect of weight ratios on the transmission properties [Fig. 3]. It is observed that the transmission of pure PMMA reduces significantly with addition of PC as transmission is found to be 75% with the addition of 10 wt% PC in PMMA. Furthermore the UV cutoff edge is shifted towards lower energy (longer wavelength), which signifies the effect of PC addition. The variation in the absorption coefficient as a function of incident energy of radiation can be expressed by the Davis and Mott relation for amorphous materials [14]:

$$\alpha h\nu = B(h\nu - E_g)^n$$

where B is the band tailing parameter, E_g is the optical band gap, $h\nu$ is the incident photon energy and the values of $n=2$, 3, 1/2 and 1/3 corresponding to indirect allowed, indirect forbidden, direct allowed and direct forbidden transitions, respectively, depending upon the nature of electronic transition responsible for the absorption. Band gap can be calculated from the linear region of the transmission curve by extrapolating them to meet the $h\nu$ axis at $(\alpha h\nu)^n=0$. Fig. 3 (inset) illustrates the dependence of $(\alpha h\nu)^2$ on the photon energy $h\nu$ for the PMMA, PC and PC:90PMMA samples. Calculations reveal a significant reduction in the band gap of PMMA film with the introduction of PC in PMMA. The band gap for PMMA is found to be 5.15 eV, while for PC:90PMMA and PC it has the values 4.57 and 3.75 eV, respectively.

Infrared spectroscopy is a useful technique to study the supramolecular interaction between the molecules. Fourier Transform Infrared (FTIR) absorption spectra of pure PC, pure PMMA and its blends with different proportions of PC and PMMA in the spectral range 400–4000 cm^{-1} are shown in Fig. 4. The fingerprint vibrations corresponding to PMMA, i.e. C–O–C symmetric stretching, O–CH_3 deformation and CH_3 asymmetric stretching vibrations, are identified at 990, 1384 and 2952 cm^{-1}, respectively. PMMA is a saturated polymeric ester (–COOR) that yields an intense and sharp band due to symmetrical stretching vibration of the carbonyl group at 1730 cm^{-1} (as shown in (Fig. 4[A]). The infrared absorption spectrum of the pure PC polymer exhibits peaks due to C–(CH_3) (827 cm^{-1}), C–O (1193 cm^{-1}), C–CH_3 symmetric (1365 cm^{-1}), in-plane C=C (1508 cm^{-1}), phenyl ring (1600 cm^{-1}), C=O (1773 cm^{-1}) and CH_3 stretch (2968 cm^{-1}) vibrations (Fig. 4[B]). The intensity of the infrared absorption due to PC is significantly lowered as the proportion of PMMA in the blend increases. The appearance of two distinct bands at 1730 and 1773 cm^{-1}, both corresponding to the C=O stretch vibration in PC:60 PMMA blend sample, shows the formation of immiscible blend at this ratio, i.e. PC and PMMA are almost independent. On increasing the concentration of PMMA (PC:90PMMA) this peak is observed to be largely shifted ($\sim$1750 cm^{-1}). This vibrational shift may result from interaction between the carbonyl groups of PMMA with the carbonate group and the phenyl ring in PC, which may be facilitated when the chains of the two polymers are close enough, as in the ultimately mixed and formed homogeneous PC:PMMA blends [15,16]. It has already been reported that PC and PMMA show some miscibility when one of the components is present in a low concentration [17]. However, the miscibility of two polymers could not be confirmed by FTIR technique as the formation of a hydrogen bond also generates a redshifted peak than the original one of the carbonyl group [18]. In our case miscibility among polymers was confirmed by DSC technique. The miscibility of these two polymers and formation of single phase is reported based on the interactions of the carbonyl and benzene group of both the polymers [19].

The IR absorption spectra of the Tb^{3+} ion doped PC:90PMMA sample show the C=O stretching vibration at 1741 cm^{-1} slightly shifted (by $\sim$9 cm^{-1}) with respect to the undoped sample. The positions of carbonyl vibration in PC:90PMMA and Tb–PC:90PMMA are found at 1750 and 1741 cm^{-1}, respectively; the redshift reveals the interaction of Tb^{3+} ion with the carboxylic group of the blend. Oxygen atom is of basic nature while Tb^{3+} is of acidic nature, possibly C=O coordinating with Tb^{3+} ion. When Tb^{3+} ion interact with Oxygen atom of the carbonyl group the electron density reduces consequently weakens the σ bond of C=O and leads to redshift corresponding to its characteristic vibration.

3.2.2. Photoluminescence spectroscopy

The photoluminescence spectra of Tb^{3+} ion doped in PC, in PMMA and in PC:90PMMA samples were recorded in the range of 400–700 nm using 355 nm radiation as an excitation source. It was observed that the Tb^{3+} ion shows stronger luminescence in the PMMA sample than in the PC sample. The luminescence intensity of the RE ion is known to be strongly affected by the phonon frequency of the host. Thus it is probably the large phonon frequency associated with the phenyl group ($\sim$1600 cm^{-1}) of PC polymer, playing a destructive role in the observed luminescence behavior. The four emission bands observed at 488, 544, 583, and 618 nm

correspond to the transitions $^5D_4 \rightarrow {}^7F_j$ ($j=6, 5, 4, 3$) of Tb^{3+} ion; the $^5D_4 \rightarrow {}^7F_5$ transition at 544 nm is the brightest. The mechanism of observed transitions can be explained as follows: the absorption peaks corresponding to intraconfigurational (4f–4f) transitions ($^7D_2$ and $^7D_3 \rightarrow {}^7F_6$) of Tb ions at 28,150 and 26,336 cm^{-1} are reported in literature [20,21]. Initially incident 355 nm (28,170 cm^{-1}) photon is resonantly absorbed and excites Tb^{3+} ion to the $^5D_2$ state, which relaxed quickly and nonradiatively to the $^5D_3$ level. Since no emission from the $^5D_3$ level to any of the low lying states (^7F_i; $i=3$, 4, 5, and 6) are not visible as the energy gap between $^5D_3$ and $^5D_4$ level is only $\sim$4500 cm^{-1}, which is comparable to the highest lattice phonon vibrations of –OH, –NH, and –CH, it seems that this state also decays nonradiatively (phonon assisted decay) to the $^5D_4$ level. Further, since the energies of $^5D_3 \rightarrow {}^7F_0$ transition and $^5D_4 \rightarrow {}^7F_6$ transition are nearly equal a cross relaxation process could occur [22]. The possible pathway of the cross relaxation process can be represented by the equation

$$Tb^{3+}(^5D_3) + Tb^{3+}(^7F_6) \rightarrow Tb^{3+}(^5D_4) + Tb^{3+}(^7F_0)$$

Excited Tb^{3+} ions in $^5D_4$ level relax radiatively to different low lying levels [^7F_j ($j=6, 5, 4, 3$)] and emit, observed colors.

Photoluminescence spectra of Tb^{3+} ions have been recorded in blends with different proportions of PC and PMMA [Fig. 5]. The maximum emission intensity is seen for the PC:90 PMMA blend. Any further decrease in the proportion of PC reduces the luminescence intensity. The blend (PC:90 PMMA) shows better performance in comparison to either of the pure polymers. The decrease in luminescence intensity with increase in PC is probably because of the formation of immiscible blend and an overall decrease in transmission **[**Fig. 3**]** [15]. The immiscibility of PC and PMMA and existence of two phases is also supported by two T_g in the thermal analysis and FTIR spectra at PC:60 PMMA.

Luminescence intensity of the Tb^{3+} ions is optimized with the $TbCl_3 \cdot 6H_2O$ concentration (1–8 wt%) in PC:90PMMA blend. It was found that the emission intensity of Tb^{3+} ions reduces considerably beyond 4 wt% of $TbCl_3 \cdot 6H_2O$, which is due to energy migration among Tb–Tb ions and commonly known as the concentration quenching phenomenon.

The luminescence decay of the transition at 544 nm in Tb doped PC:PMMA sample has been studied at room temperature. The measured lifetime (τ_{meas}) for the $^5D_4 \rightarrow {}^7F_5$ transition has been determined from the decay curve, which is represented by the following equation:

$$I = I_0 A\, e^{(-t/\tau)}$$

where A is the amplitude and τ is the fluorescence lifetime. Decay curve for Tb^{3+} ion in a PC:90 PMMA blend can be fitted to a single exponential and the lifetime is calculated to be $\sim$580 μs (Fig. 6).

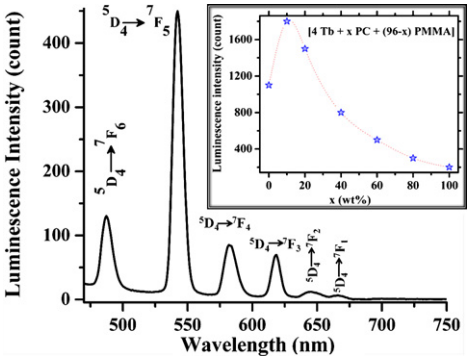

Fig. 5. Photoluminescence spectrum of 4 wt% Tb^{3+} ion doped PC:90 PMMA blend under excitation with 355 nm. A variation in integrated emission intensity of $^5D_4 \rightarrow {}^7F_5$ transition (544 nm) with the PC concentration in PMMA while the Tb^{3+} ion concentration was kept constant.

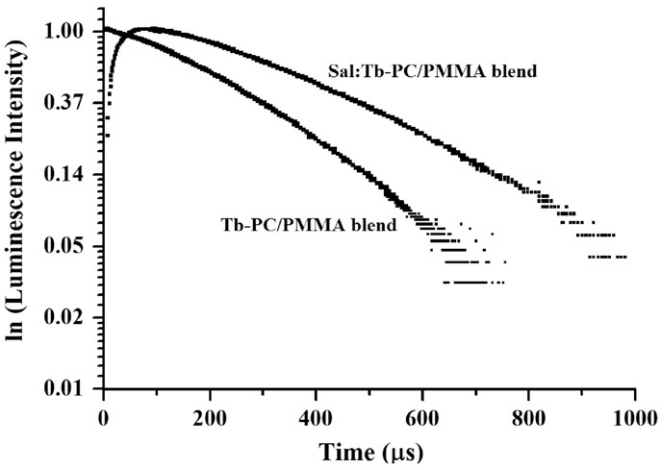

Fig. 6. Decay curves of $^5D_4 \rightarrow {}^7F_5$ transition (544 nm) of Tb^{3+} ion in PC:90 PMMA and in Sal:Tb–PC:90 PMMA samples.

The lifetimes for the same transition in the hosts PC:60 PMMA and PC:80 PMMA are measured to be $\sim$410 and $\sim$520 μs, respectively, showing a decreasing trend with increasing PC concentration. This means that non-radiative relaxation increases with the PC concentration.

3.3. *Spectroscopic study of Tb–PC:PMMA blend with salicylic acid:*

Interest in lanthanide complexes with aromatic carboxylic acid, which are used as a structural and functional probe in biological systems, is growing rapidly. Salicylic acid (o-hydroxybenzoic acid) [hereafter called Sal] is one of the few such compounds that provide simultaneously the advantage of chelation as well as sensitization to the RE ions. Yang and Zhang [23] studied the photoacoustic spectra of lanthanide complexes with Sal and reported that the phenolic –OH and carboxylic –COOH groups take part in chelate formation with the Tb^{3+} ions, resulting in a more stable complex. Some polymers have been demonstrated to be capable of wrapping around the metal cations, causing dramatic changes in its surroundings and shielding to the central metal ion from deactivation of O–H oscillators [24]. Considering the synergetic effect of rare earth ions coordinating with polymers and ligands, it is worthwhile to synthesize RE organic ligands complexes in polymer with specific luminescence properties.

The excitation spectra of $TbCl_3$ and Tb:Sal codoped PC:PMMA sample have been recorded corresponding to the $^5D_4 \rightarrow {}^7F_5$ transition of Tb^{3+} ion to observe any possibility of energy transfer from Sal to Tb^{3+} **[**Fig. 7**]**. A broad ($\sim$100 nm wide) and intense band in the range 265–360 nm is observed in the codoped sample, which is absent when only Tb is doped in the PC:PMMA blend. A significant excitation intensity is observed corresponding to the 355 nm wavelength from Tb^{3+} ion. The excitation band corresponding to the Tb^{3+} ion transition shows that Sal is an effective sensitizer by transitions $n \rightarrow \pi^*$ and $n \rightarrow n^*$.

Photoluminescence from Tb^{3+} ions codoped with Sal in PC:PMMA blend excited by 355 nm laser radiation is shown in Fig. 8. PC:PMMA blend sample containing Sal shows an intense and wide emission band centered at 450 nm. When Sal was added to Tb–PC:90 PMMA the intensity of all the emission peaks of Tb^{3+} ion is increased systematically. This enhancement is due to energy transfer from excited Sal to Tb^{3+} ion. When 4 wt% of Sal is present in the codoped polymer the emission intensity shows an increase by 2 orders of magnitude as compared to the sample containing only Tb. The increase in intensity of the Tb peaks is a

clean indication of energy transfer. Furthermore, a few new transitions $^5D_3 \rightarrow {}^7F_{3,2,1}$ also appear for the codoped sample that were not visible in $TbCl_3 \cdot 6H_2O$ doped PC:90PMMA sample. The shielding of 4f orbitals by valence shell of 5s and 5p orbital causes the f–f absorption bands to be narrow [25]. The FWHM of the blue (488 nm), green (544 nm), yellow (583 nm) and red (618 nm) bands are 11.2, 9.5, 12.1, and 8.7 nm, respectively. The narrow FWHM of the bands improves the color purity, which is highly desirable in display devices.

Color is a psychophysical property of the human eye and it needs to be expressed mathematically for precision. It is found that the response of the human eye can be mathematically expressed well in terms of CIE coordinates given by International Commission for Illumination (CIE, Commission Internationale de l'Eclairage) [26,27]. It involves parameters x and y to specify the chromaticity, which covers the properties hue and saturation on a two dimensional chromaticity diagram. The chromaticity coordinates were calculated for samples doped with Tb and with sal:Tb samples and are (0.36, 0.42) and (0.37, 0.44), respectively. The color correlated temperature was 4773 K for the Sal:Tb sample. The schematic energy level diagram and the possible energy transfer pathways suggested by the present study are shown in Fig. 9.

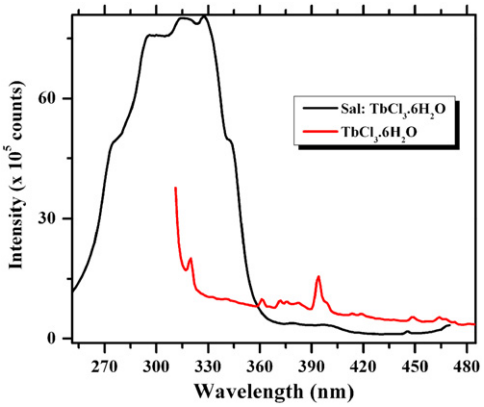

Fig. 7. Excitation spectra of $TbCl_3 \cdot 6H_2O$ and Sal: $TbCl_3 \cdot 6H_2O$ doped in PC:90 PMMA blend corresponding to the $^5D_4 \rightarrow {}^7F_5$ transition of Tb^{3+} ion.

For the effective energy transfer between donor and acceptor a reasonable overlapping of the emissions of donor and absorption of acceptor is essential. Furthermore, the direct coordination of Sal to Tb^{3+} ion improves the energy transfer efficiency due to reduced donor–acceptor distance.

The energy transfer mechanism in the present case can be explained by the singlet and the triplet state positions of Sal reported at 34,482 and 23,300 cm^{-1}, respectively [28], which is in perfect overlap with the region of ^5D_j, ^5L_j states of Tb^{3+} ions. Tb^{3+} ions have poor absorption compared to Sal in UV–blue region; hence Sal absorbs large 355 nm photons. The UV laser photon was initially absorbed by Sal to excite it to the S_1 state, which may decay to the lowest triplet state T_1 through intersystem crossing. This may give a weak triplet–singlet emission. Sal molecule in both S_1 and T_1 states can transfer energy to Tb^{3+} ions [29]: (1) S_1 energy level overlap with the energy levels in the region of ^5D_j, ^5L_j states of Tb^{3+} ions. From S_1 it is the $^5D_1$ state that is

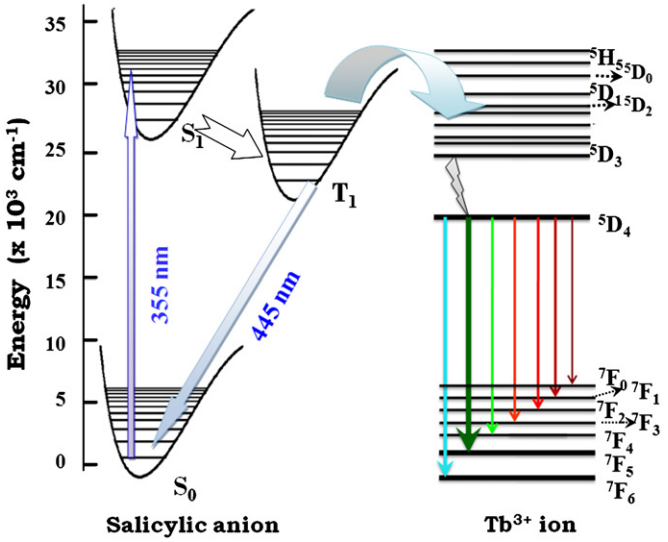

Fig. 9. Schematic energy level diagram and the possible energy transfer path ways among salicylic acid and Tb^{3+} ions under excitation at 355 nm.

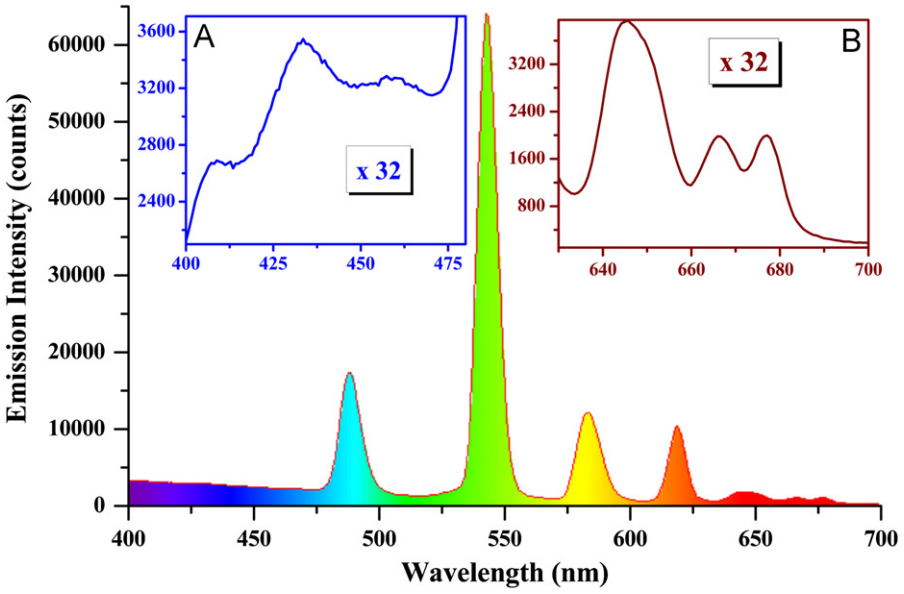

Fig. 8. Photoluminescence spectra of Sal:Tb codoped PC:90PMMA blend. Insets of figure are the enlarged (× 32) portions of 400–490 and 630–700 nm for clarity of the transitions.

directly excited and decays through two step $^5D_2 \rightarrow {}^5D_3$ and $^5D_3 \rightarrow {}^5D_4$ to the state from which the fluorescence is observed. In contrast the sal molecule in T_1 directly excites the $^5D_4$ state of Tb^{3+}. Both of these mechanisms may be in operation simultaneously. According to Ref. [30], the intra-molecular energy transfer from the lowest triplet energy state is more effective and is responsible for the excellent luminescence properties of lanthanide chelates. The intra-molecular energy transfer efficiency calculated is 80%, using the ratio of the peak area of donor [31]. The higher emission intensity observed in Sal–Tb–PC:90 PMMA sample is due to the transfer of most of its absorbed energy, from Sal to Tb^{3+} ions.

To understand the luminescence dynamics of the Sal:Tb–PC:90 PMMA sample, the decay curves for the $^5D_4 \rightarrow {}^7F_5$ transition (544 nm) have been recorded [Fig. 6]. The curve has been expressed by the following function:-

$$N(t) = A[\exp(-t/\tau_d) - \exp(t/\tau_r)]$$

where A is a constant and τ_d and τ_r are the decay and rise times, respectively.

The existence of a small rise time ($\sim$18 μs) is indicative of an additional channel for exciting the upper state (instead of resonance absorption of 355 nm photon by Tb^{3+} ions). This additional mechanism is through non-radiative energy transfer from sal, whose absorption cross-section for the incident light is large to the Tb^{3+} ion. The lifetime of the Tb^{3+} ion in the presence of the salicylic acid is seen to be substantially large (710 μs) as compared to its value when sal is not present (580 μs). Enlargement of decay time reflects the non-radiative energy transfer from salicylic acid to the lanthanide ion.

4. Conclusion

Structural, thermal and spectroscopic properties of Tb–PC: PMMA blend were investigated using different techniques. As evidenced by UV–vis and FTIR spectroscopy, interaction of Tb^{3+} ion with the C=O bond is suggested. PC:90 PMMA blend was found to be a suitable host for Tb^{3+} ion luminescence. Miscibility of the two polymers is observed in PC:90PMMA blend composition, which correlates with the luminescence result. Concentration quenching effect was observed beyond 4 wt% of Tb concentration. Enhancements in Tb^{3+} ion fluorescence were observed if salicylic acid is added in the blend through energy transfer from Sal to Tb^{3+} ions. This has been verified with measurement of the fluorescence decay curve.

Acknowledgements

The authors are thankful to Professor Dhananjai Pandey, School of Materials Science and Technology, Institute of Technology (BHU) for fruitful discussion. They want to acknowledge the instrumentation support provided by Dr. H. Mishra to record the emission spectrum. Dr. Y. Dwivedi and Mr. A.K. Singh acknowledge Council of Scientific and Industrial Research, New Delhi, India, for Senior Research Fellowship.

References

[1] A.J. Kenyon, Prog. Quantum. Electron. 26 (2002) 225.
[2] J. Zubia, J. Arrue, Opt. Fiber Technol. 7 (2001) 101.
[3] H. Ma, A.K.Y. Jen, L.R. Dalton, Adv. Mater. 14 (2002) 1339.
[4] A.P.B. Sinha, in: C.N.R. Rao, J.R. Ferraro (Eds.), Spectroscopy in Inorganic Systems, vol. 2, Academic, New York, 1971.
[5] A. Rosendo, M. Flores, G. Cordoba, R. Rodríguez, R. Arroyo, Mater. Lett. 57 (2003) 2885.
[6] Y. Agari, A. Ueda, Y. Omura, S. Nagai, Polymer 38 (1997) 801.
[7] G.D. Butzbach, J.H. Wendorff, Polymer 32 (1991) 1155.
[8] J.S. Chiou, J.W. Barlow, D.R. Paul, J. Polym. Sci. Part B: Polym. Phys. 25 (1987) 1459.
[9] P. Viville, O. Thoelen, S. Beauvois, R. Lazzaroni, G. Lambin, J.L. Bredas, K. Kolev, L. Laude, Appl. Surf. Sci. 86 (1994) 411.
[10] T. Kyu, J.M. Saldanha, Macromolecules 20 (1987) 2840.
[11] R. Bonzanini, D.T. Dias, E.M. Girotto, E.C. Muniz, M.L. Baesso, J.M.A. Caiut, Y. Messaddeq, S.J.L. Ribeiro, A.C. Bento, A.F. Rubira, J. Lumin. 117 (2006) 61.
[12] R. Bonzanini, E.M. Girotto, M.C. Goncalves, E. Radovanovic, E.C. Muniz, A.F. Rubira, Polymer 46 (2005) 253.
[13] G. Kaur, Y. Dwivedi, S.B. Rai, J. Fluoresc. 21 (2011) 423.
[14] N.F. Mott, E.A. Davis, Electronic. Processes. in Non-Crystalline. Materials, 2nd edition, Clarendon, Oxford, 1979.
[15] T.K. Kyu, C.C. Ko, D.S. Lim, D.S. Noda, J. Polym. Sci. Polym. Lett. Ed. 31 (1993) 1641.
[16] K.C. Kim, D.R. Paul, Macromolecules 25 (1992) 3097.
[17] W.N. Kim, C.M. Burns, Macromolecules 20 (1987) (1876).
[18] P.C. Painter, Y. Park, M.M. Coleman, Macromolecules 21 (1988) 66.
[19] W.T. Carnell, P.R. Fields, K. Rajnak, J. Chem. Phys. 49 (1968) 4447.
[20] L. Armelao, S. Quici, F. Barigelletti, G. Accorsi, G. Bottaro, M. Cavazzini, E. Tondello, Coord. Chem. Rev. 254 (2010) 487.
[21] Z.G. Garland, Polymer Blends and Composite in Multi Phase Systems, in: C.D. Han (Ed.), ACS Advances in Chemistry Series No. 206, American Chemical Society, Washington DC., 1984.
[22] G.C. Kim, T.W. Kim., S.-I. Mho, S.G. Kim, H.L. Park, J. Korean Phys. Soc 34 (1999) 97.
[23] Y.T. Yang, S.Y. Zhang, Spectrochem. Acta A 60 (2004) 2065.
[24] Y. Okamoto, J. Kido, H.G. Brittain, S. Paoletti, J. Macromol. Sci. Chem. 25 (1988) 1385.
[25] Q. Li, T. Li, J.G. Wu, J. Phys. Chem. B 105 (2001) 12293.
[26] Y. Dwivedi, A. Rai, S.B. Rai, J. Appl. Phys. 104 (2008) 043509.
[27] 〈www.hyperphysics.phy-astr.gsu.edu/hbase/vision/cie.html〉.
[28] G. Qian, M.Q. Wang, J. Chin. Ceram. Soc. 26 (1998) 331.
[29] J. Sun, W. Xie, L. Yuan, K. Zang, Q. Wang, Mater. Sci. Eng. B 64 (1999) 157.
[30] M. Latva, H. Takalo, V.M. Mukkala, C. Matachescu, J.C.R. Ubis, J. Kankare, J. Lumin. 75 (1997) 149.
[31] J.R. Lakowicz, Principles of Fluorescence Spectroscopy, Plenum Press, New York, 1983.